LBL-37474
UC-401
Preprint

Lawrence Berkeley Laboratory

UNIVERSITY OF CALIFORNIA

CHEMICAL SCIENCES DIVISION

Submitted to Journal of Chemical Physics

Dynamics of the Acetylene-d_2, Ethylene-d_4, and Tetradeuteromethane Products from the Reaction of D-Atoms with a Graphite Surface

L.A. Smoliar, C.L. Berrie, and Y.T. Lee

July 1995

REFERENCE COPY
Does Not
Circulate
Bldg. 50 Library.
LBL-37474
Copy 1

Prepared for the U.S. Department of Energy under Contract Number DE-AC03-76SF00098

DISCLAIMER

This document was prepared as an account of work sponsored by the United States Government. While this document is believed to contain correct information, neither the United States Government nor any agency thereof, nor the Regents of the University of California, nor any of their employees, makes any warranty, express or implied, or assumes any legal responsibility for the accuracy, completeness, or usefulness of any information, apparatus, product, or process disclosed, or represents that its use would not infringe privately owned rights. Reference herein to any specific commercial product, process, or service by its trade name, trademark, manufacturer, or otherwise, does not necessarily constitute or imply its endorsement, recommendation, or favoring by the United States Government or any agency thereof, or the Regents of the University of California. The views and opinions of authors expressed herein do not necessarily state or reflect those of the United States Government or any agency thereof or the Regents of the University of California.

LBL-37474
UC-401

Dynamics of the Acetylene-d_2, Ethylene-d_4, and Tetradeuteromethane Products from the Reaction of D-Atoms with a Graphite Surface

L.A. Smoliar, C.L. Berrie, and Y.T. Lee

Department of Chemistry
University of California, Berkeley

and

Chemical Sciences Division
Lawrence Berkeley Laboratory
University of California
Berkeley, California 94720

July 1995

This work was supported by the Office of Naval Research Grant No. N00014-89-J-1297, through the U.S. Department of Energy under Contract No. DE-AC03-76SF00098.

Dynamics of the Acetylene-d_2, Ethylene-d_4, and Tetradeuteromethane Products from the Reaction of D-Atoms with a Graphite Surface

L. A. Smoliar,* C. L. Berrie, and Y. T. Lee

Department of Chemistry, University of California, Berkeley
and
Chemical Sciences Division, Lawrence Berkeley Laboratory, Berkeley, CA 94720

Abstract

The dynamics of the reaction products produced by a supersonic beam of D-atoms impinging on the basal plane of a graphite surface were investigated by measuring the time-of-flight spectra of individual reaction products evolving from the surface at specific angles between the atomic beam and the surface plane (with the source-to-detector angle fixed at 90°). Translational energy distributions derived from the time-of-flight spectra indicate that there is a barrier in the exit channel for the formation and subsequent desorption of acetylene-d_2, ethylene-d_4, and tetradeuteromethane. In addition, by varying the angle, θ_i, between the atomic beam and the surface plane, knowledge of the surface reaction mechanism is obtained, indicating that tetradeuteromethane is formed both via the Eley-Rideal mechanism and the Langmuir-Hinshelwood mechanism while acetylene-d_2 and ethylene-d_4 results from the Langmuir-Hinshelwood mechanism.

*Present address: No. 1, R&D Road VI, Hsinchu Science-Based Industrial Park, Synchrotron Radiation Research Center SRRC, Hsinchu, Taiwan 30077

Introduction

Thermodynamic and kinetic aspects of the reaction of hydrogen atoms with graphite have been studied extensively. Early experiments were performed in a bulb by heating the graphite or by passing molecular hydrogen gas over a hot graphite filament or rod to adsorb atomic hydrogen, and then measuring the desorbing gases. The uptake and desorption of H_2 was studied[1] as well as formation and desorption of hydrocarbon species such as CH_4 and C_2H_2.[2] Later, the kinetics of the reaction of hydrogen atoms with a graphite surface was studied by dissociating molecular hydrogen in a radiofrequency discharge source. In the surface temperature range of 450-1200 K, the products found were molecular hydrogen and methane.[3] Using the technique of modulated molecular beams, Balooch et. al. studied the reaction of H-atoms with graphite where the H-atoms were produced in a pyrolytic effusive source.[4] They found that for surface temperatures up to 800 K, methane was the only product, but acetylene was seen at temperatures above 1000 K. They proposed a model in which the methane was formed by sequential addition of adsorbed H-atoms and the acetylene was formed by surface recombination of CH groups. They did not see any other hydrocarbon products, in particular ethylene, which differs from this work.

While the kinetics of the reacion of H-atoms with graphite have been well studied, the dynamics have not been directly explored. The dynamics in such hydrogen-carbon systems are now of interest, particularly in the related area of diamond growth. In this work, a supersonic beam of D-atoms incident on the basal

plane of a graphite surface is used to generate reaction products whose individual velocities are directly measured upon evolution from the surface. By varying the angle, θ_i, between the beam and the surface plane, while the beam-to-detection angle remains fixed at 90°, a distribution of products giving insight into the reaction mechanism is obtained. The dynamics of the deuterated acetylene, ethylene, and methane products are examined. Two reaction mechanisms occur: methane is formed both through the Eley-Rideal and Langmuir-Hinshelwood mechanisms while the acetylene and ethylene are formed through the Langmuir-Hinshelwood mechanism.

Experimental

A continuous supersonic beam of D-atoms was directed towards the basal plane of highly oriented pyrolitic graphite (HOPG) maintained at T_{surf}= 570 K or T_{surf}= 705 K in a gas-surface scattering apparatus, described previously.[5] The products of the surface reaction are chopped by a cross-correlation wheel, mass selected, and counted by a channeltron after travelling through a flight distance of 23.9cm.[6] The time-of-flight spectra of individual mass-selected reaction products were measured for m/e= 32, 30, 28, 26, 20, 18, 16, and 14. In addition, the reflected beam was monitored.

The surface was mounted on a 3-axis rotatable manipulator equipped with a resistive heater. The HOPG graphite sample was obtained from Union Carbide (grade ZYH monochromator) and heated for at least 24 hours in vacuum (1×10^{-7}

torr) to T_{surf}= 720-770 K before running an experiment. Surface temperature was limited to a narrow range because of concerns about absorption of background gases and limits of the crystal heater. In the range studied, no surface temperature dependence on the dynamics was clearly seen. Time-of-flight spectra were measured as a function of θ_i, the angle between the source and the surface plane, with the source-to-detector angle fixed at 90°. In such a configuration, any memory of the incident beam in the product dynamics is readily ascertained, but it is not possible to measure a full flux angular distribution to determine energy scaling. In addition, by using a D-atom source, differentiation between deuterium from the beam and hydrogen from the bulk crystal[4] is possible.

A D-atom source with a flux of ~5 x 10^{18} atoms cm^{-2} s^{-1}, previously described,[7] was used to prepare D-atoms by thermal pyrolysis of D_2. D_2 does not react with graphite,[4] so the atomic species is the true reactant species. In a previous experiment on the H and D atom reactions with LiF(001) to make HF and DF, respectively, an artifact in the time-of-flight spectra due to collisional ionization was identified and discussed extensively.[7] The same effect is observed in some of the time-of-flight spectra for the D-atom reactions with graphite, and similarly discounted. The collisional ionization arises from the fact that D^+, metastable D_2, and Rydberg D-atoms are all produced in the electron bombardment ionizer and can collisionally ionize other molecules in the region between the ionizer and the quadrupole filter of the detector.[8-11] Because the collisional process leads to broadening, which is dependent on θ_i and the particular m/e setting of the

quadrupole, there is no systematic way to subtract this artifact from the data. Thus, it is simply excluded from the fitting when analyzing the reaction product data.

Results

Product time-of-fight spectra were taken for m/e= 32, 30, 28, 26, 20, 18, 16, and 14. Table I lists the assignments of the fragments detected. Signal was not observed above m/e= 32, indicating that C_2 is the longest chain hydrocarbon, and no evidence for the evolution of radical species such as CD, CD_2, or CD_3 was found.[4] Radical species would be expected to evolve from the surface more slowly than the stable molecular products observed. Additionally, because no time-of-flight peak was observed at m/e= 36, ethane-d_6 is not a product. The three hydrocarbon products observed were deuterated acetylene, ethylene, and methane. The products will hereafter be referred to by these names with the deuteration understood. The fragmentation patterns for these products and ethane are listed in Table II.[12]

By considering the fragmentation patterns, two schemes for fitting the data were devised and tested, one assuming the C_2 species is ethylene and the other assuming it is ethane. The scheme involving ethane did not fit the data well,[13] and in addition, since m/e= 36 signal was not observed (which is unique to the ethane product), this possibility can be ruled out. Thus, only one scheme, where the C_2 species is ethylene, is discussed here.

The first step of the fitting scheme comes from the fact that C_2D_4 and C_2D_2 do not fragment in the electron bombardment ionizer to m/e= 20. Thus, m/e= 20 data can be fit at all θ_i to derive a single translational energy distribution describing CD_4 evolution. In addition, the fit to the m/e= 18 time-of-flight peak should be generated from the same translational energy distribution since m/e= 18 only appears in the fragmentation pattern of CD_4. Fig. 1 shows the time-of-flight data for m/e= 20 and 18 taken at θ_i= 30°, along with a fit derived from the translational energy distribution in Fig. 2. The fit is a simulated time-of-flight spectrum obtained by the forward convolution method, which includes the various apparatus functions affecting the data.[14-16] Fig. 3 shows how the translational energy distribution of Fig. 2 fits the data at θ_i= 20°, 45°, and 60° for two different surface temperatures, T_{surf}= 570 K and T_{surf}= 705 K. In the θ_i= 45° and 60° data, the fast peak is discounted as an artifact from collisional ionization.[7] There does not seem to be an appreciable difference in the time-of-flight spectra with surface temperature within the narrow range studied here.

Next, the m/e= 32 data, attributed solely to C_2D_4, is fit at all angles θ_i to generate a single translational energy distribution. This is the distribution describing the dynamics of ethylene evolving from the surface. The fit for m/e= 32 at four angles θ_i is shown in Fig. 4, and the corresponding translational energy distribution is in Fig. 5. The m/e= 26 data has two contributions, one from C_2D_4, and the other from C_2D_2. Once the C_2D_4 distribution has been determined from the m/e= 32 data, the translational energy distribution of C_2D_2 is adjusted to generate

the best total fit to the m/e= 26 data at all angles θ_i, while also finding the relative contributions of the two channels. The fit for θ_i= 20°, 45°, and 60° is shown for two surface temperatures in Fig. 6. Once again, the time-of-flight data do not show a dependence on T_{surf} in the range studied. The acetylene translational energy distribution used to fit the m/e= 26 data is shown in Fig. 7.

The time-of-flight spectra at m/e= 16 and 14 should be fit with a combination of the translational energy distributions already derived for methane, ethylene, and acetylene. In the case of m/e= 16, the data can be fit using a combination of the distributions for ethylene and methane; acetylene only gives a small amount of m/e= 16 upon fragmentation in the ionizer. The m/e= 16 data is shown in Fig. 8 with a fit generated from a combination of the translational energy distributions for methane, Fig. 3, and ethylene, Fig. 5. Data for m/e= 14 is fit using a combination of all three translational energy distributions found above, Fig. 9. The contribution from methane is negligible, which is at first surprising when only considering the fragmentation pattern of the different products. It turns out that methane is the minor product of the gas-surface reaction under the conditions used, though, as will be discussed later. Therefore, it is reasonable that the methane contribution is negligible compared to acetylene and ethylene in the m/e= 14 time-of-flight spectrum. Finally, data at m/e= 30 must be a result of ethylene fragmenting in the electron bombardment ionizer. In Fig. 10, time-of-flight data taken for m/e= 30 is shown for θ_i= 20° with a fit generated from the ethylene translational energy distribution in Fig. 5.

In Fig. 11, the three translational energy distributions used to fit the data are plotted with a Maxwell-Boltzmann distribution for T_{surf}= 705 K. The distributions for the products clearly peak at higher energies than the Maxwell-Boltzmann distribution, indicating that there is a barrier to desorption of the product molecules. For the product translational energy distributions, $<E>_T$= 3.1 kcal/mole for ethylene, $<E>_T$= 4.1 kcal/mole for acetylene, and $<E>_T$= 3.9 kcal/mole for methane. The $<E>_T$ for acetylene and methane is nearly the same, and the shapes of the distributions are similar, but the low-energy side of the acetylene distribution is shifted to higher energy as is the peak, by about 0.5 kcal/mole. It turns out that the methane distribution is reflecting the translational energy release from two different surface reaction mechanisms, which will be addressed in a discussion of the θ_i product distributions. Since the mechanism of acetylene and methane formation is different, as evidenced by the θ_i distributions (see below), the similarity of the two translational energy distributions is probably just coincidental. Ethylene has E_{max}~9 kcal/mole, which is lower than the common E_{max}~11 kcal/mole for acetylene and methane.[17]

Qualitatively, the yield of the products under the conditions used indicates that the major product is ethylene and the minor product is methane. However, the relative yield of products is expected to be dependent on the D-atom flux and so no attempt to quantify a branching ratio is made here. The flux of D-atoms used in this experiment is about 100 times higher than in the modulated molecular beam work of Balooch et. al. (where ethylene product was not observed),[4] suggesting that

ethylene formation is dependent on the availability of D-atoms.

The θ_i distributions for each product were measured, and the results are plotted in Figs. 12-14 in polar form along with a cos(θ) distribution, which is scaled to the product intensity for $\theta_i = 45°$. For the θ_i distribution, it is important to remember that the beam-to-detector angle remains fixed at 90°, and thus the normal component of the D-atom incident energy changes with θ_i. The cos(θ) distribution shown here would be observed if the product: 1) was in thermal equilibrium with the surface at the surface temperature and 2) had no "memory" of the incident beam. In Figs. 12-14 the beam is incident on the surface between $\theta_i =$ 0-90°, and the products are detected from $\theta =$ 90-180° as shown. The angle θ_i is thus equal to the angle between the detector and the surface normal for each measurement. The acetylene θ_i distribution (Fig. 12) is most similar to a cos(θ) distribution. The ethylene θ_i distribution is somewhat similar to a cos(θ) distribution, except the product intensity is more strongly peaked toward the surface normal (Fig. 13). Methane, however, differs from the acetylene and ethylene; part of its distribution is strongly peaked toward 45° and part looks like a $\cos^n(\theta)$ distribution (Fig. 14). The θ_i distributions show that some of the methane product has a "memory" of the incident beam, while all of the acetylene and ethylene products do not. The important dynamical implications of this result will be discussed in the following section.

Discussion

Product Translational Energy

The translational energy and θ_i distributions of the deuterated methane, acetylene, and ethylene products reveal some dynamical and mechanistic aspects of the gas-surface reaction. The importance of considering both the energy released into translation and the angular distribution of products has been demonstrated.[18] Measuring an angular distribution gives insight into the reaction mechanism and desorption dynamics, but can be misleading without an accompanying translational energy distribution. This is particularly true when a cos(θ) angular distribution is observed, which is normally associated with thermal desorption but can also arise simply from the way a molecule's energy is accommodated at the surface before desorption (i.e. partitioned between the directions parallel and perpendicular to the surface).

The translational energy distributions in Fig. 11 have been normalized to have the same area. All three peak at higher energies than a Maxwell-Boltzmann distribution for T_{surf}= 705 K (shown) and of course for T_{surf}= 570 K (not shown). This is indicative of a barrier in the exit channel of each potential energy surface governing the interaction of individual products with the graphite surface.[19] If the exit channels had no barrier, Maxwell-Boltzmann distributions would be expected. Deviations from Maxwell-Boltzmann behavior characteristic of $T_{surface}$ have been observed in many studies of desorption.[20-22] In fact, Comsa has pointed out that there is really no general reason to expect to see Maxwell-Boltzmann distributions for the desorption of molecules from a surface.[23] The distributions can be loosely

characterized by a "temperature"($T_{<E>} = <E>_T/2k_B$, where k_B is the Boltzmann constant) to quantify the deviation from $T_{surface}$; $T_{<E>} = T_{surface}$ in the case of a Maxwell-Boltzmann distribution.[24] For ethylene, acetylene, and methane, $T_{<E>}$ = 780, 1032, and 982 K, respectively.

The three product distributions are also wider than a Maxwell-Boltzmann distribtution. As the newly formed product surmounts the barrier and leaves the surface, potential energy is not only channelled into translation but also into internal modes of the product, which is reflected in the width of the derived translational energy distribution. Products with less translational energy are more internally excited. The width can also reflect reaction at different types of surface sites, which will effectively change the total available energy to the departing molecule. For the two products that desorb without a memory of the incident beam, the width is larger for ethylene, which has more degrees of freedom than acetylene (i.e. more ways to partition internal energy). The methane is formed through two mechanisms, a direct reaction and a surface recombination, and the combination of the two mechanisms or reaction from different types of surface sitess may broaden the distribution.

The ethylene distribution has the lowest $T_{<E>}$ (780 K) and also has a lower E_{max} of ~9 kcal/mole. Such behavior is consistent with a lower barrier height with respect to the final product state in the exit channel for the ethylene product as compared to the acetylene or methane. The fact that ethylene was found to be the major product under the conditions used also suggests a lower barrier in the

forward direction, from the reactants to the transition state. The ratio of products ethylene: acetylene: methane is ~9:3:1. The barrier in the exit channel can result from the geometric and configurational requirements of the transition state for a particular product to form and evolve. In the case of ethylene, the carbon has the same sp^2 hybridization of the graphitic carbon on the surface. Perhaps this explains why ethylene evolution would have a lower barrier.

Product θ_i Distributions

The θ_i distributions in Figs. 12-14 illustrate how the product flux changes when the surface is rotated. In the rotating surface, fixed source-detector arrangement, the normal component of the incident D-atom energy varies with θ_i. Thus, the distribution observed cannot be properly fit to a $\cos^n(\theta)$ distribution unless there is no effect from the incident beam. However, in the case of acetylene the distribution clearly shows a loss of "memory" of the incident beam. It is interesting to note, in fact, that the angle with the most product intensity here is from the measurement where the D-atom has the least incident energy in the normal direction. A mechanistic picture whereby two CD groups move around on the surface, find each other, and join together to evolve as acetylene is consistent with no "memory" of the beam, which is the Langmuir-Hinshelwood type mechanism.[25] The plotted $\cos(\theta)$ distribution, shown for comparison, is what would be seen if a true thermal desorption were occurring with the product in equilibrium with the surface. However, since the translational energy distribution

clearly peaks at higher energy than a Maxwell-Boltzmann distribution, thermal desorption is not an appropriate description of the desorption dynamics. The observed θ_i distribution must arise from the dynamics of the last formation step and exit off the surface, reflecting the shape of the exit barrier in the potential energy surface. While the CD groups are accomodated to the surface, the newly formed acetylene is not, for there is no surface temperature dependence observed. The acetylene product formation and desorption can be a concerted process, resulting in a very short residence time for the acetylene on the surface. Thus the $\cos(\theta)$ distribution reflects the way the acetylene's energy is divided in the directions parallel and perpendicular to the surface as it moves through the exit channel of the potential energy surface.

The θ_i distribution for ethylene, Fig. 13, also shows a loss of "memory" of the beam. The distribution is more highly peaked toward the normal than a $\cos(\theta)$ distribution, as shown. In fact, it can be fit to a $\cos^{2.6}(\theta)$ distribution, again based on loss of "memory" of the incident beam. The translational energy distribution already indicates that the ethylene evolution is not a simple thermal desorption. A microscopic picture of two accomodated CD_2 groups diffusing along the surface until they find each other and form the product is consistent with the angular distribution, which is again the Langmuir-Hinshelwood mechanism. However, the strong peaking indicates that the exit channel barrier has a different shape than that in the acetylene case. This barrier is more significant along the normal direction. The ethylene product, whose dynamics show no surface temperature dependence, is

not accomodated to the surface. In addition, its energy must be partitioned more in the direction perpendicular to the surface than parallel to the surface in order to result in the $\cos^{2.6}(\theta)$ distribution. Peaked angular distributions have been previously interpreted as resulting from excess energy in the desorbing molecule in a study of CO_2 formed by reaction of CO and oxygen (O_2^{2-} and O) on a Pt(111) surface.[26] There may be a particular configuration of the transition state that leads to more energy in the coordinate normal to the surface.

Fig. 14 shows the θ_i distribution for the methane product. Methane differs from acetylene and ethylene: it appears that two mechanisms, Eley-Rideal and Langmuir-Hinshelwood, are operating simultaneously. One part of the distribution is highly peaked toward 45°, indicating that there is a "memory" of the incident beam. This part of the angular picture is consistent with D-atom addition from the beam to radical species adsorbed on the surface: first to $CD_{(ads)}$, then to $CD_{2(ads)}$, and finally to $CD_{3(ads)}$, constituting an Eley-Rideal mechanism. Sequential additions from adsorbed D-atoms or D-atoms that have suffered a few collisions with the surface before reaction (and therefor lost information about their incident coordinates) contribute to the other part of the angular distribution, which has a $\cos^{3.4}(\theta)$ distribution. The $\cos^{3.4}(\theta)$ contribution is from reactions of the Langmuir-Hinshelwood type mechanism. Thus, both the Eley-Rideal and Langmuir-Hinshelwood mechanisms are occuring simultaneously. Unfortunately, it is not possible to deconvolute the translational energy distribution (Fig. 2) to reflect the individual contributions from the two mechanisms. Reports of the Eley-Rideal

mechanism are quite rare, and so the observation of such a mechanism in this case is of particular interest.[27-29] From kinetic studies,[4] the addition to CD_2 is expected to be the rate-determining step while the addition to CD_3 is very fast. Thus, if there is a competition between D-atom addition to CD_3 and two CD_3 groups finding each other on the surface to form ethane, the D-atom addition would be favored. Perhaps this is why no evidence for ethane formation has been observed.

Microscopic Picture

In the present study, the observed products were methane, acetylene, and ethylene. While methane and acetylene were reported previously in a modulated molecular beam study,[4] ethylene was not. Possible explanations for this discrepancy are that the flux of D-atoms is two orders of magnitude higher here, and the D-atoms are produced in a supersonic expansion with $E_{incident}$~ 7.5 kcal/mole. Previously, acetylene formation was only seen at high surface temperatures (above 1000 K), and methane was the only hydrocarbon product at lower temperatures (up to 800 K). This suggests that the surface temperature had to be high enough to insure mobility of the $CD_{(ads)}$ species on the surface so that they could find each other with a reasonable frequency. The incident beam energy of ~7.5 kcal/mole is well above k_BT_{surf} at 1000 K (k_BT_{surf}= 1.99 kcal/mole), so there may be ample energy available for mobility of newly formed species, depending on how much energy is consumed in the initial reaction. Thus, the incident energy from the D-atom can be partially accommodated by CD and CD_2

mobility at the surface, which is necessary for recombination reactions to form acetylene and ethylene.

In further considering the mobility of the radical species at the surface, it becomes clear why ethane formation is not favored. The graphitic carbon atom starts as an sp^2 carbon, covalently bound to three other carbon atoms. As D-atom addition occurs, one C-C bond is broken and a D-atom is attached. However, a CD species is still anchored to the surface by two other C-C bonds if the sp^2 hybridization is maintained. Likewise, a CD_2 species is anchored by one C-C bond. A CD_3 species loses its anchor, though, if sp^2 hybridization is maintained, and thus may not remain on the surface long enough to recombine with another CD_3 group. The final D-atom addition quickly forms CD_4, and thus CD_3 may be a very short-lived species under conditions of high D-atom flux. This would explain the absence of ethane product. In addition, radical species evolution would probably be unfavorable.

Comparison with other Molecular Beam Etching Studies

The dynamics of only a few etching reactions have been studied using molecular beam-surface scattering. Some are mentioned here for the sake of comparison in order to gain a better understanding of the dynamics observed in the D-atom/graphite system. Of particular interest is why some systems show barrierless thermal desorption behavior and others do not.

The dynamics of Cl_2 etching of GaAs have been studied. In one

experiment, the etching of the GaAs(110) surface to form $GaCl_3$ was reported,[30] with $GaCl_3$ evolution well described by a Maxwell-Boltzmann distribution with a temperature below $T_{surface}$ and a cosine angular distribution. These results were attributed to an absence of an activation barrier for desorption. In another experiment,[31] time-of-flight spectra of the GaCl from Cl_2 reacting with GaAs(100) were measured. A cosine distribution for GaCl was observed, and the authors mention that an even better fit was found for $\cos^{1.5}(\theta)$, i.e. more peaked towards the surface normal than $\cos(\theta)$. The time-of-flight spectrum was wider than a Maxwell-Boltzmann distribution (the width was dependent on $T_{surface}$ with slower products appearing at lower surface temperatures) except at a high surface temperature of 550 °C. Attempts to fit the time-of-flight distribution for GaCl by including a factor accounting for a surface residence time were unsuccessful. It was postulated, however, that GaCl comes from different types of defect sites, giving rise to different residence times and thus broadens the time-of-flight distribution.

The velocities of $SiCl_n$ (n= 2, 3 and 4) reaction products from the reaction of Cl_2 with Si(111) were measured.[19] The product time-of-flight distributions were well fit with Maxwell-Boltzmann distributions with temperatures 9.0% higher than $T_{surface}$. In addition, the angular distribution was a bit peaked toward the normal, fit by $\cos^{1.26}(\theta)$. The $SiCl_2$ results were explained in terms of a low potential barrier in the exit channel resulting in translational heating of the newly formed products upon desorption.

The results presented here show broader product distributions than expected for a Maxwell-Boltzmann distribution as in the GaCl work, which could arise for similar reasons, i.e. reaction and desorption from different types of surface sites. In addition, the ethylene θ_i distribution is more highly peaked towards the normal than a cos(θ) distribution as observed for the $SiCl_2$ and also the GaCl. The acetylene distribution follows cos(θ) well, but the translational energy distribution shows that thermal desorption is not taking place. As in the case of $SiCl_2$ formation and desorption, there is a barrier in the exit channel for each product, indicated by the translational energy distribution peaking at higher energy than a Maxwell-Boltzmann distribution for the surface temperature.

Conclusion

The dynamics of three hydrocarbon reaction products in the reaction of D-atoms with a graphite surface have been explored. Time-of-flight measurements of individual products coupled with variation of the beam-surface angle allow for determination of the translational energy imparted to each product and the role of the incident beam in each product's formation on the surface. Unlike some other etching reactions reported in the literature, the products do not evolve by a simple thermal desorption process. In fact, there is a barrier in the exit channel for each product, and thus the translational energy distribution is shifted to higher energies than a Maxwell-Boltzmann distribution for the surface temperature. Additionally, the distributions do not have the functional form of a Maxwell-Boltzmann

distribution. By examining the influence of the incident D-atom beam, it was determined that the methane was formed both by sequential addition of D-atoms from the beam to radical species on the surface (Eley-Rideal mechanism) and also through a Langmuir-Hinshelwood type mechanism, while acetylene and ethylene were formed by recombination of accommodated CD and CD_2 species on the surface, respectively (Langmuir-Hinshelwood). The accommodation of the incident energy allows for surface mobility and the radical species lose "memory" of the incident D-atom velocity. The major product was ethylene under the conditions of D-atom flux and incident energy used. A study of the branching ratio of products by varying the D-atom flux would be interesting and would allow for a greater understanding of the competition between the pathways leading to the three observed products.

Acknowledgements

LAS thanks Professor T. J. Chuang, Dr. J. C. Lin, and Professor D. R. Olander for helpful discussions as well as AT&T Bell Laboratories for a Ph.D. Scholarship. This project was supported by the Office of Naval Research through Dr. Richard Miller.

References and Notes

[1]J. P. Redmond and P. L. Walker, Jr., J. Phys. Chem. **54**, 1093 (1960).

[2]J. T. Clarke and B. R. Fox, J. Chem. Phys. **46**, 827 (1967).

[3]B. J. Wood and H. Wise, J. Phys. Chem. **73**, 1348 (1969).

[4]M. Balooch and D. R. Olander, J. Chem. Phys. **63**, 4772 (1975).

[5]Paper submitted to J. Chem. Phys..

[6]R. David, K. Kern, P. Zeppenfeld, and G. Comsa, Rev. Sci. Instrum. **57**, 2771 (1986).

[7]Paper submitted to J. Chem. Phys..

[8]L. D. Weaver and R. H. Hughes, J. Chem. Phys. **52**, 2299 (1970).

[9]V. Cermak, J. Chem. Phys. **44**, 1318 (1966).

[10]D. W. Koopman, J. Chem. Phys. **49**, 5203 (1968).

[11]H. Hotop, F. W. Lampe, and A. Niehaus, J. Chem. Phys. **51**, 593 (1969).

[12]E. Stenhagen, S. Abrahamsson, and F. W. McLafferty, Atlas of Mass Spectral Data (John Wiley and Sons, New York, 1969).

[13]A fitting scheme assuming that m/e=32 was due to ethane did not fit the data well. In particular, one consistent translational energy distribution could not be found to fit the m/e=26 data.

[14]A. M. Wodtke, Ph. D. Thesis, University of California, Berkeley, 1986.

[15]X. Zhao, Ph. D. Thesis, University of California, Berkeley, 1988.

[16]CMLAB2 fitting program written by J. D. Myers.

[17]The uncertainty at the tail end of the translational energy distribution from the 5msec resolution of the chopper (double sequence cross-correlation wheel) is ~1 kcal/mole.

[18]S. T. Ceyer, W. L. Gutherie, T. H. Lin, and G. A. Somorjai, J. Chem. Phys. **78**, 6982 (1983).

[19]H. Yoshikawa and K. Shobatake, Chem. Phys. Lett., **223**, 341 (1994).

[20]C. T. Rettner, E. K. Schweizer, and C. B. Mullins, J. Chem. Phys. **90**, 3800 (1989).

[21]C. R. Arumainayagam, R. J. Madix, M. C. McMaster, V. M. Suzawa, and J. C. Tully, Surf. Sci. **226**, 180 (1990).

[22]L. A. DeLouise, J. Chem. Phys. **94**, 1528 (1991).

[23]G. Comsa and R. David, Surf. Sci. Rep. **5**, 145 (1985).

[24]While $T_{<E>} = <E>_T/2k_B$ is only strictly valid for a Maxwell-Boltzmann distribution, it is often used loosely to quantify deviations in the data from a Maxwell-Boltzmann distribution. See Ref. 23.

[25]J. I. Steinfeld, J. S. Francisco, and W. L. Hase, Chemical Kinetics and Dynamics (Prentice Hall International, Inc., London, 1989) p.196.

[26]T. Matsushima, Surf. Sci., **123**, L663 (1982).

[27]M. L. Yu and L. A. DeLouise, Surf. Sci. Rep. **19**, 285 (1994).

[28]E. W. Kuipers, A. Vardi, A. Danon, and A. Amirav, Phys. Rev. Lett. **66**, 116 (1991).

[29]C. T. Rettner, Phys. Rev. Lett. **69**, 383 (1992).

[30]L. A. DeLouise, J. Chem. Phys. **94**, 1528 (1991).

[31]P. Bond, P. N. Brier, J. Fletcher, P. A. Gorry, and M. E. Pemble, Chem. Phys. Lett., **208**, 269 (1993).

Figure Captions

Fig. 1 Time-of-flight data (circles)taken at θ_i=30° for (a) m/e=20 and (b) m/e=18. The fit (solid line) is a simulated time-of-flight generated from the translational energy distribution in Fig. 2 for both (a) and (b).

Fig. 2 Translational energy distribution for tetradeuteromethane obtained by fitting m/e=20 data at all angles θ_i (some fits are shown in Fig. 3).

Fig. 3 Data (circles) taken for m/e=20 at different angles θ_i. The left side (a, c, and e) were measured with T_{surf}=570 K. The right side (b, d, f) were measured with T_{surf}=705 K. The collisional ionization component is shown (dotted line) in (c)-(f) (not a fit) and is off the scale of the graph. The simulated time-of-flight (solid line) is generated from the translational energy distribution in Fig. 2. The same translational energy distribution is used to fit all the data (a)-(f), for both surface temperatures.

Fig. 4 Data (circles) taken at m/e=32 for different angles θ_i and T_{surf}=570K. The fit (solid line) is a simulated time-of-flight spectrum generated from the translational energy distribution in Fig. 5.

Fig. 5 Translational energy distribution for ethylene-d_4 obtained by fitting m/e=32 data at all angles θ_i (some fits are shown in Fig. 4).

Fig. 6 Data (circles) taken at m/e=26 for different angles θ_i and two surface temperatures: T_{surf}=570 K (a, c, and e) and T_{surf}=705 K (b, d, and f). The collisional ionization component (off the scale of the graph) is shown in (c)-(f) (dotted line) (not a fit). The simulated time-of-flight spectra used to fit the product time-of-flight peaks are generated from the translational energy distributions of Fig. 5 (ethylene-d_4, solid line) and Fig. 7 (acetylene-d_2, dashed line). The total fit is also shown(thick line).

Fig. 7 Translational energy distribution for acetylene-d_2 obtained by fitting m/e=26 data at all angles θ_i (some fits are shown in Fig. 6).

Fig. 8 Data (circles) taken at m/e=16 for different angles θ_i. The fit is generated from the translational energy distributions for ethylene-d_4 (solid line) (Fig. 5) and acetylene-d_2 (dashed line) (Fig. 7). T_{surf}=570 K for (a), (c), and (d) and T_{surf}=705 K for (b). In (d) the collisional ionization component (off the scale of the graph) is shown (dotted line) (not a fit).

Fig. 9 Data (circles) taken at m/e=14 and θ_i=25° for T_{surf}=705 K. The ethylene-d_4 component (dotted line), the acetylene-d_2 component (solid line), and the tetradeuteromethane component (dashed line), which is negligible, are shown. The translational energy distributions of Figs. 2, 5, and 7 were used for tetradeuteromethane, ethylene-d_4, and acetylene-d_2, respectively, in fitting.

Fig. 10 Data (circles) taken for m/e=30, θ_i=20°, and T_{surf}=570 K. The fit (solid line) is a simulated time-of-flight spectrum generated from the translational energy distribution in Fig. 5.

Fig. 11 The translational energy distributions of Figs. 2 (tetradeuteromethane, dotted line), 5 (ethylene-d_4, dashed line), and 7 (acetylene-d_2 dash-dot line) are plotted with a Maxwell-Boltzmann distribution for T_{surf}=705K (solid line).

Fig. 12 The measured θ_i distribution for acetylene-d_2 (■) is plotted in polar form with a cos(θ) distribution (●) for comparison. T_{surf}=705 K.

Fig. 13 The measured θ_i distribution for ethylene-d_4 (■) is plotted in polar form with a cos(θ) distribution (●) for comparison. T_{surf}=705 K. The data is best fit with a $\cos^{2.6}(\theta)$ distribution, also shown (solid line).

Fig. 14 The measured θ_i distribution for tetradeuteromethane (■) is plotted in polar form with a cos(θ) distribution (●) for comparison. T_{surf}=705 K. Part of the tetradeuteromethane product shows a "memory" of the beam by peaking near θ_i=45°.

Table I. Assignment of Detected Ions from Reaction

m/e	parent ion assignment
32	$C_2D_4^+$
30	$C_2D_4^+$
28	$C_2D_4^+$ $C_2D_2^+$
26	$C_2D_2^+$ $C_2D_4^+$
20	CD_4^+
18	CD_4^+
16	CD_4^+ $C_2D_4^+$ $C_2D_2^+$
14	$C_2D_2^+$ CD_4^+ $C_2D_4^+$

Table II. Fragmentation Patterns[a]

m/e	Ethane-d_6 C_2D_6	Ethylene-d_4 C_2D_4	Acetylene-d_2 C_2D_2	Tetra-deutero-methane CD_4
36	185			
34	146			
32	**1000**	**1000**		
30	273	618		
28	209	640	406	
27			807	
26		106	**1000**	
24		32	286	
20				**1000**
18				830
16	54	110	13	125
14	24	64	136	72
12			194	
2				30

[a]Data from Ref. 12.

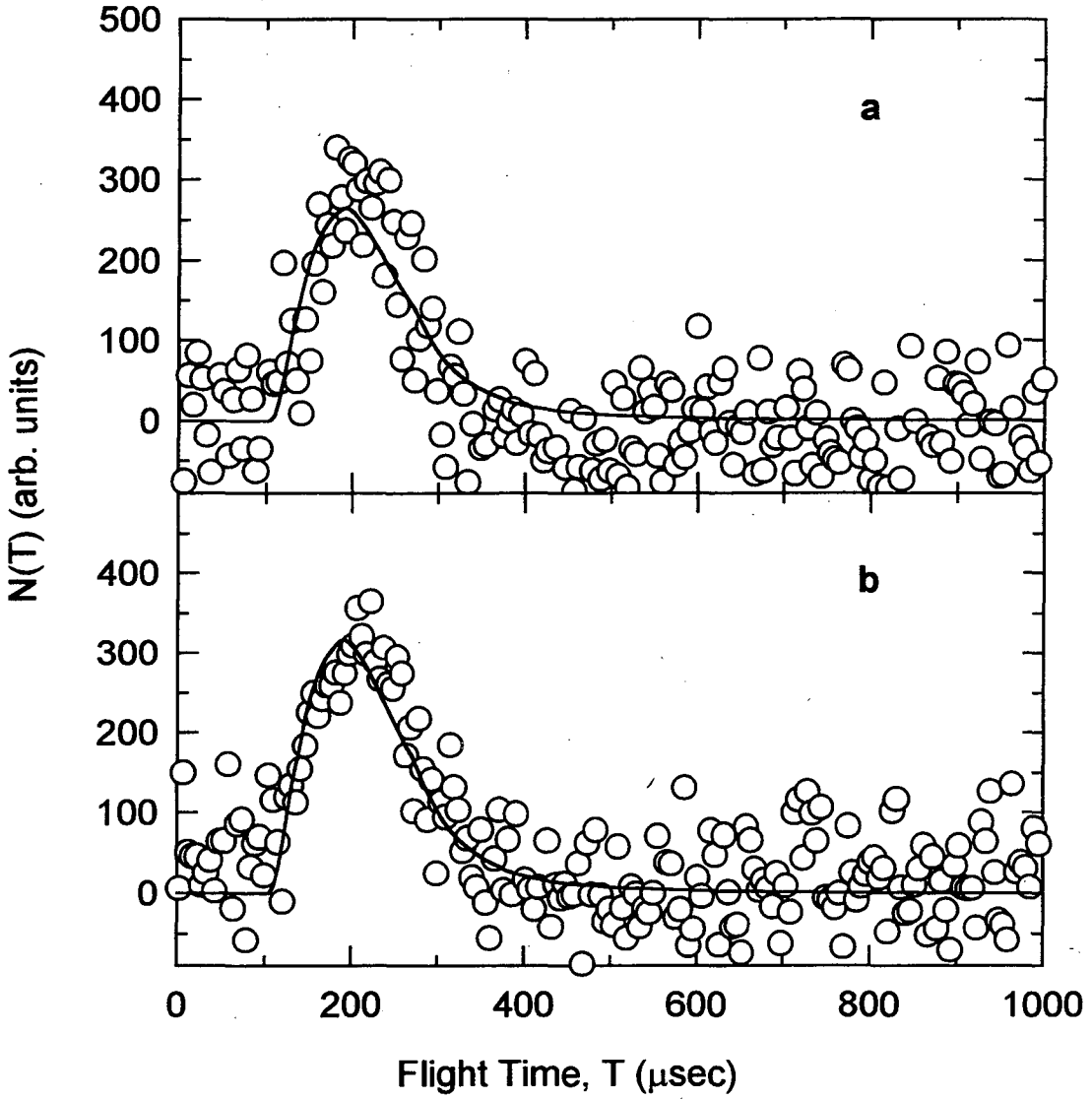

Fig. 1, L. A. Smoliar, J. Chem. Phys.

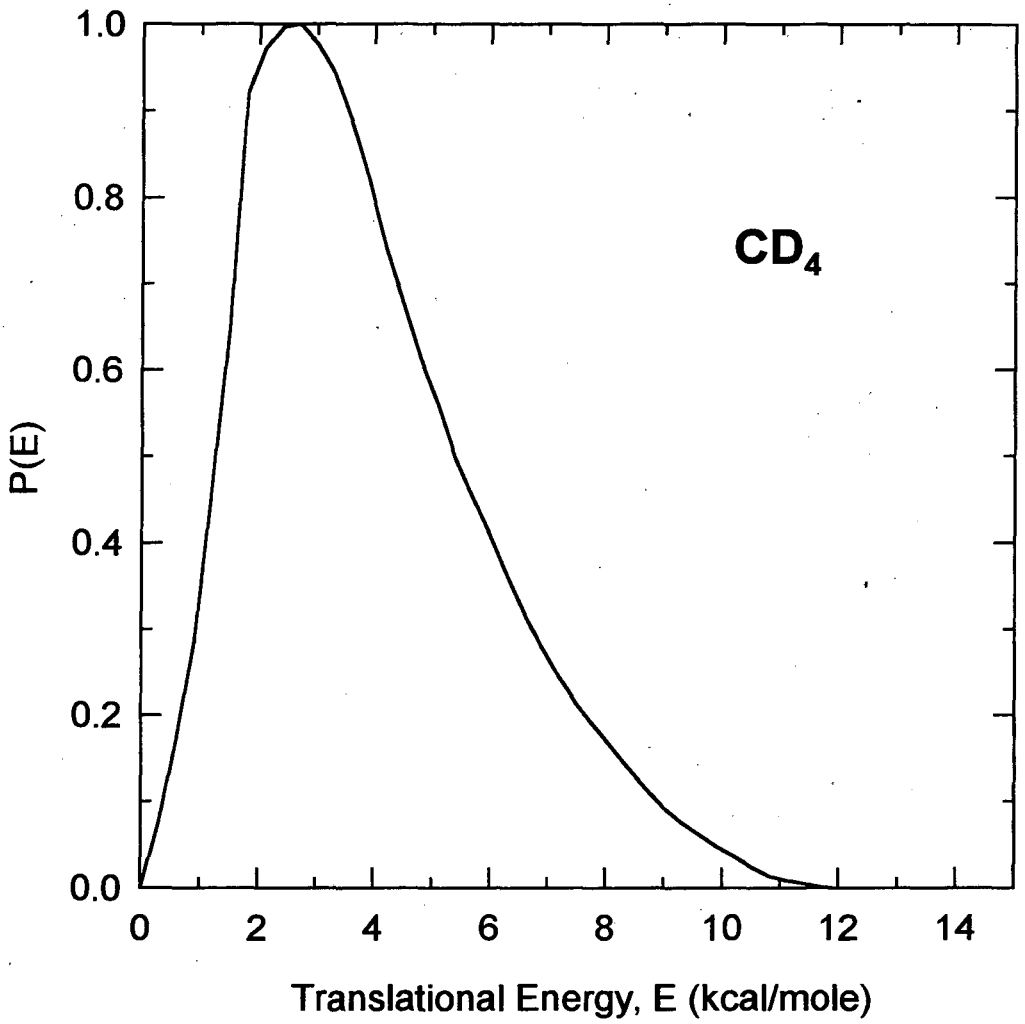

Fig. 2, L. A. Smoliar, J. Chem. Phys.

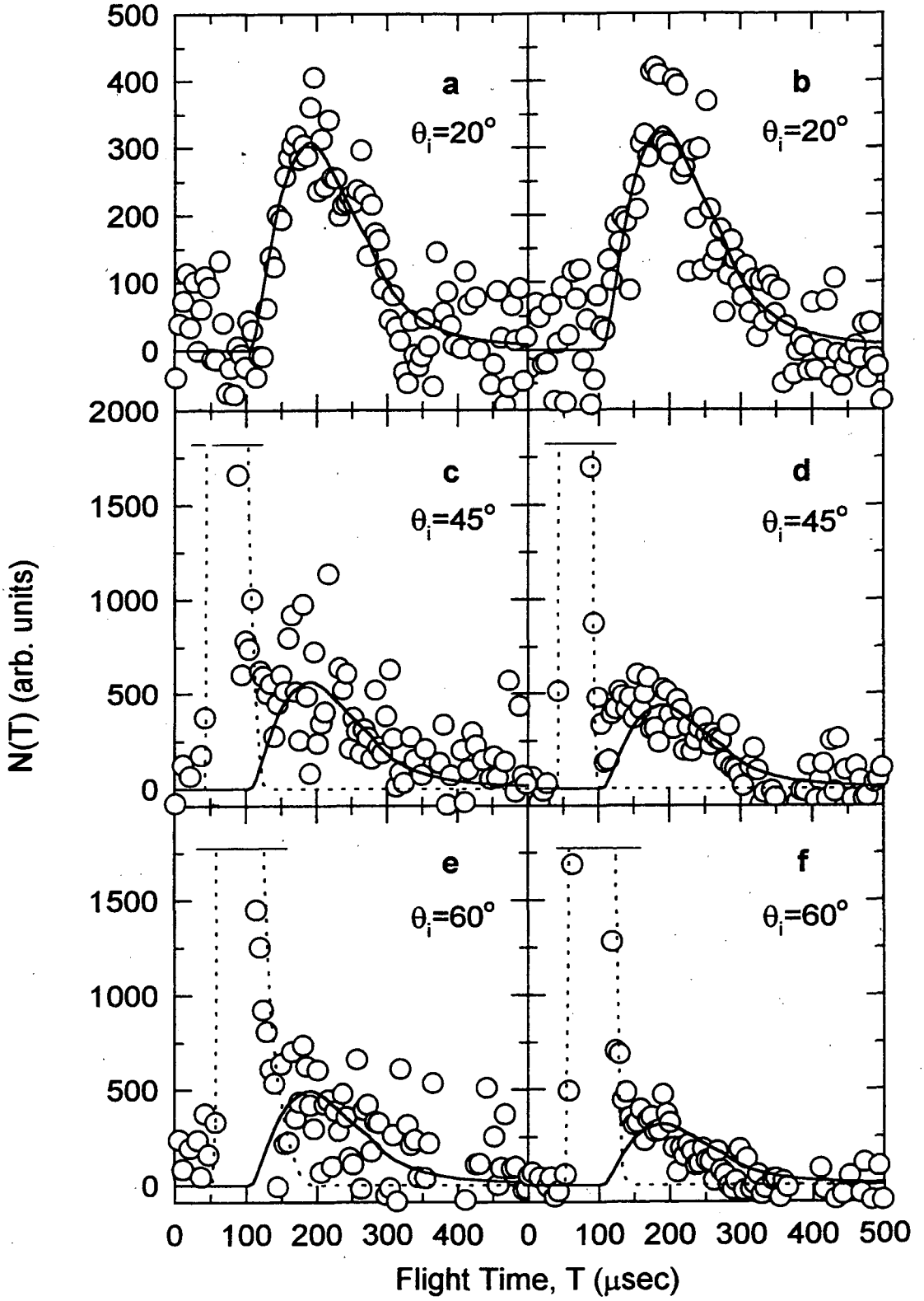

Fig. 3, L. A. Smoliar, J. Chem. Phys.

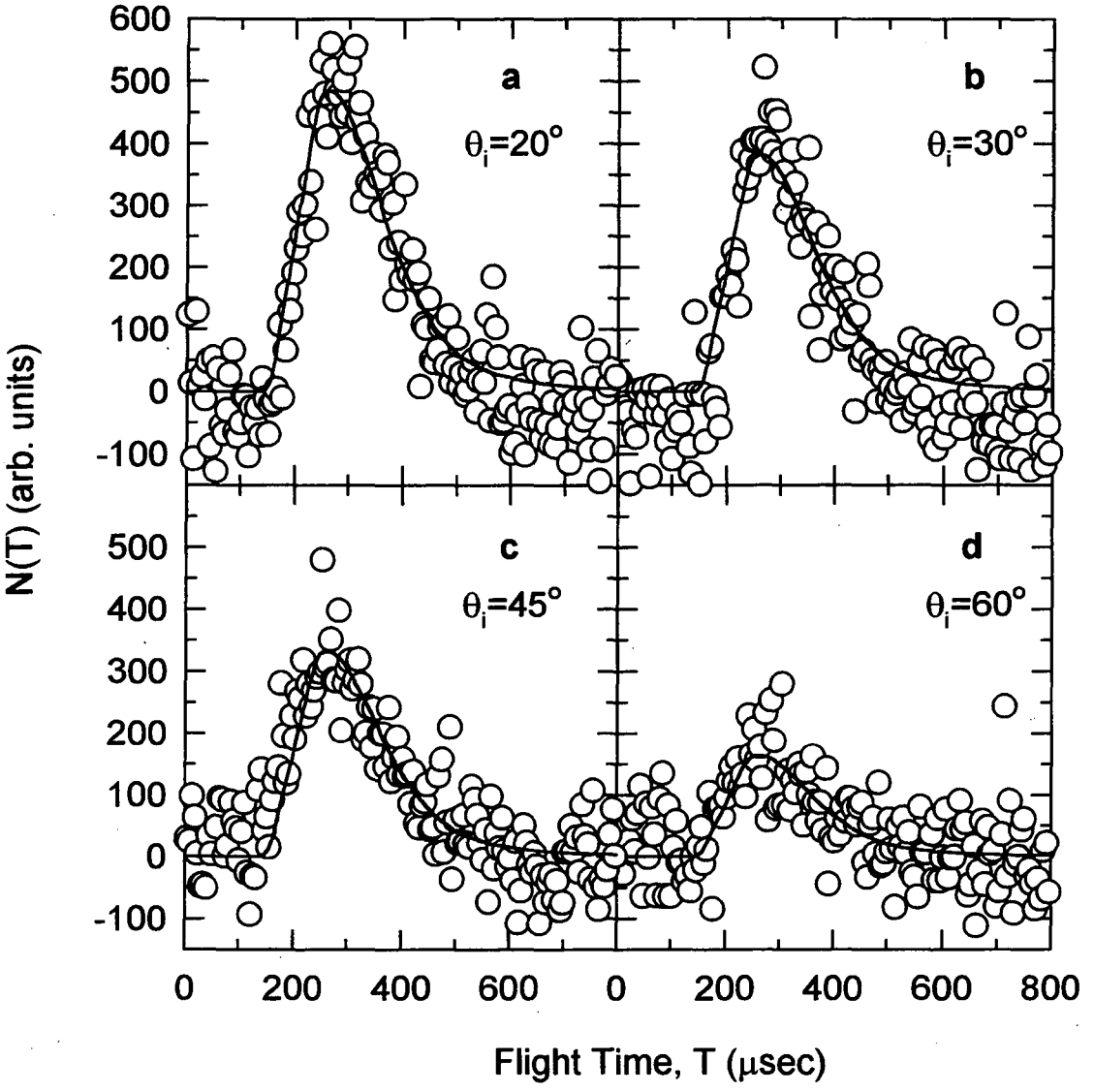

Fig. 4, L. A. Smoliar, J. Chem. Phys.

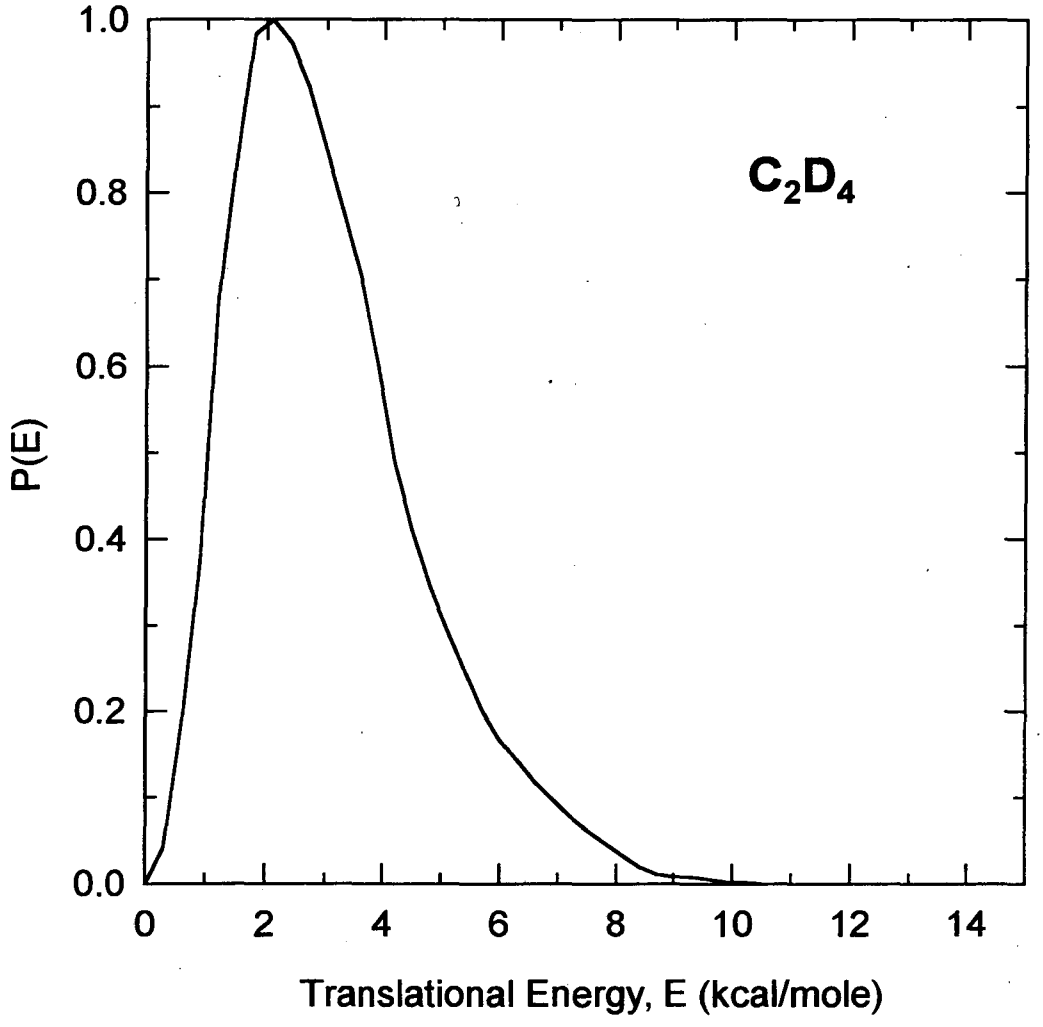

Fig. 5, L. A. Smoliar, J. Chem. Phys.

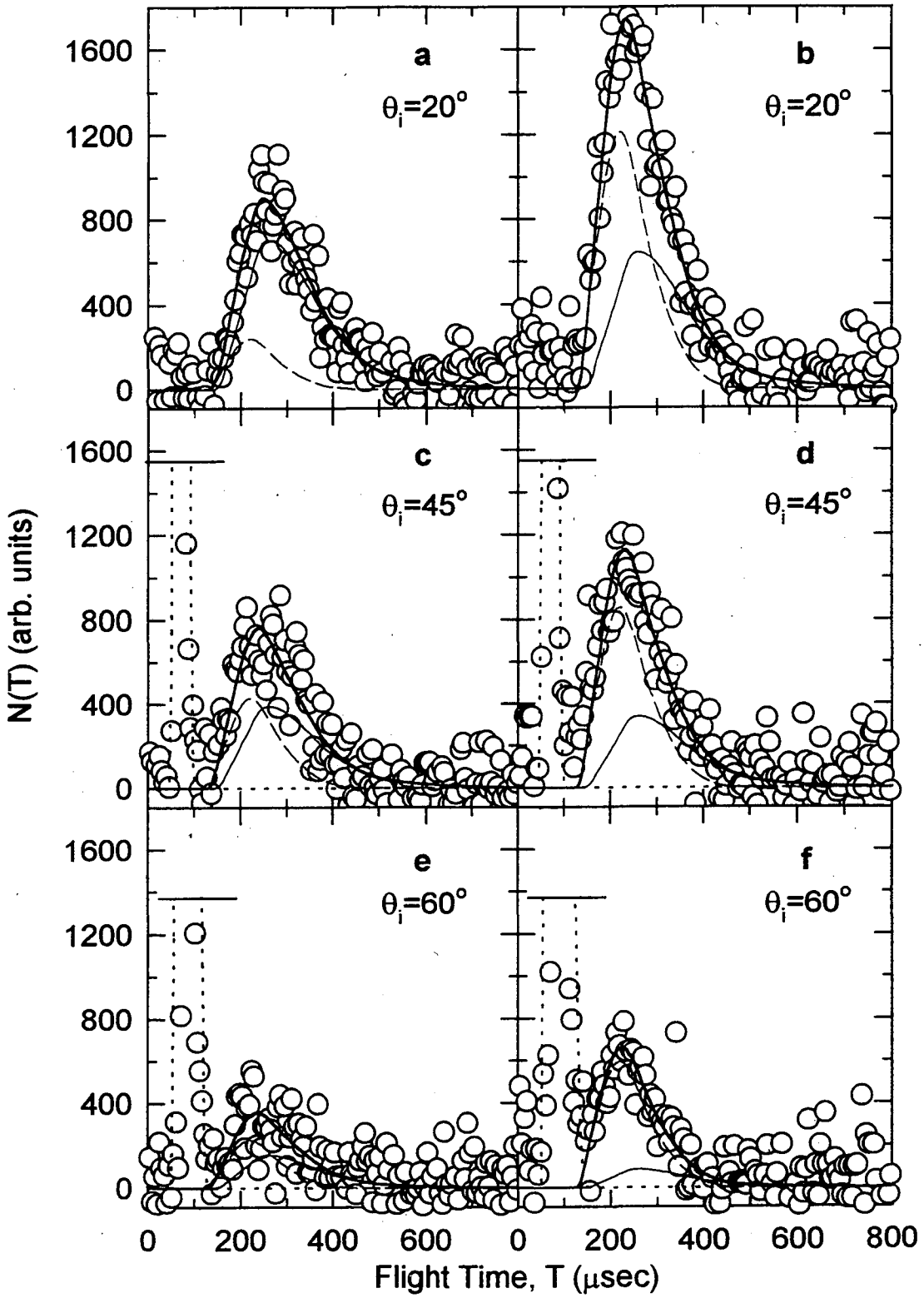

Fig. 6, L. A. Smoliar, J. Chem. Phys.

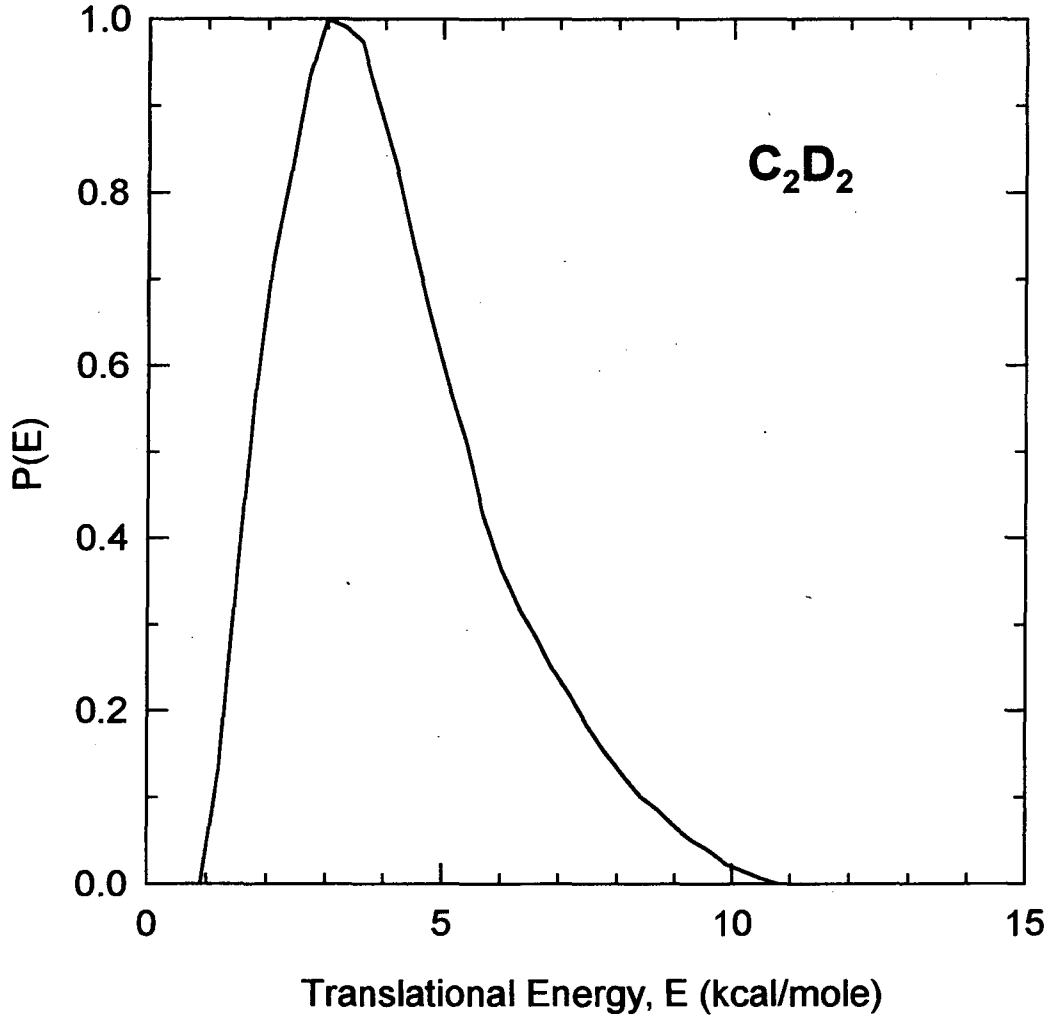

Fig. 7, L. A. Smoliar, J. Chem. Phys.

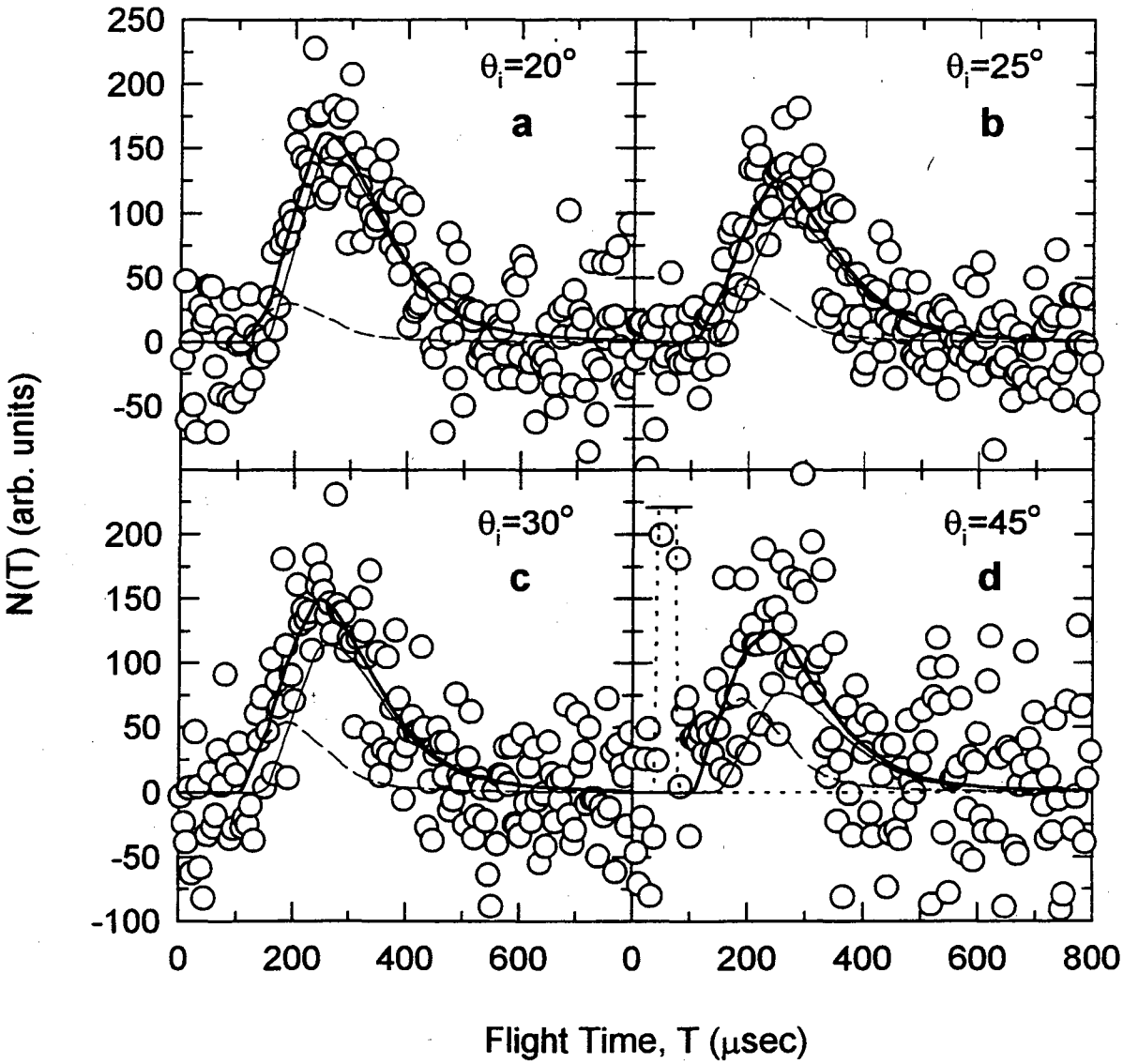

Fig. 8, L. A. Smoliar, J. Chem. Phys.

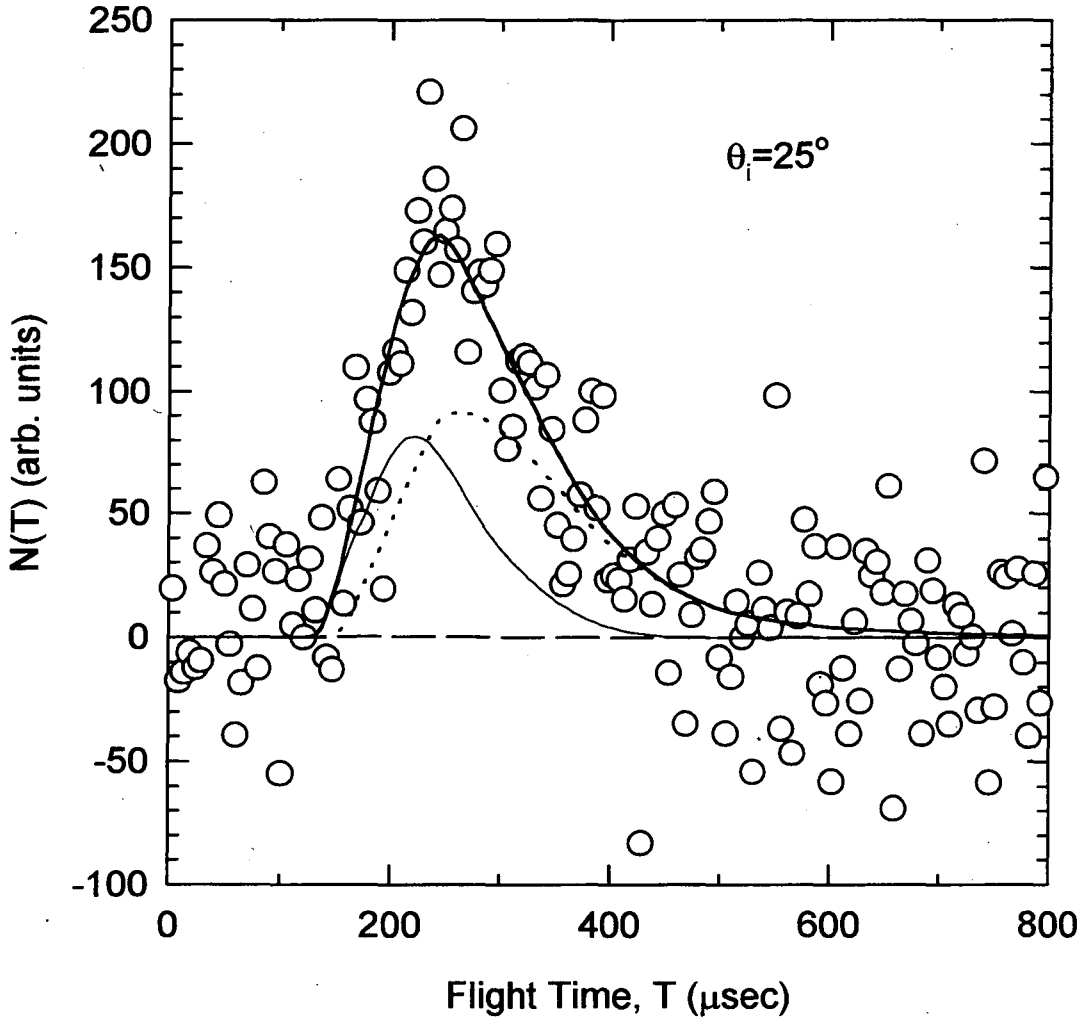

Fig. 9, L. A. Smoliar, J. Chem. Phys.

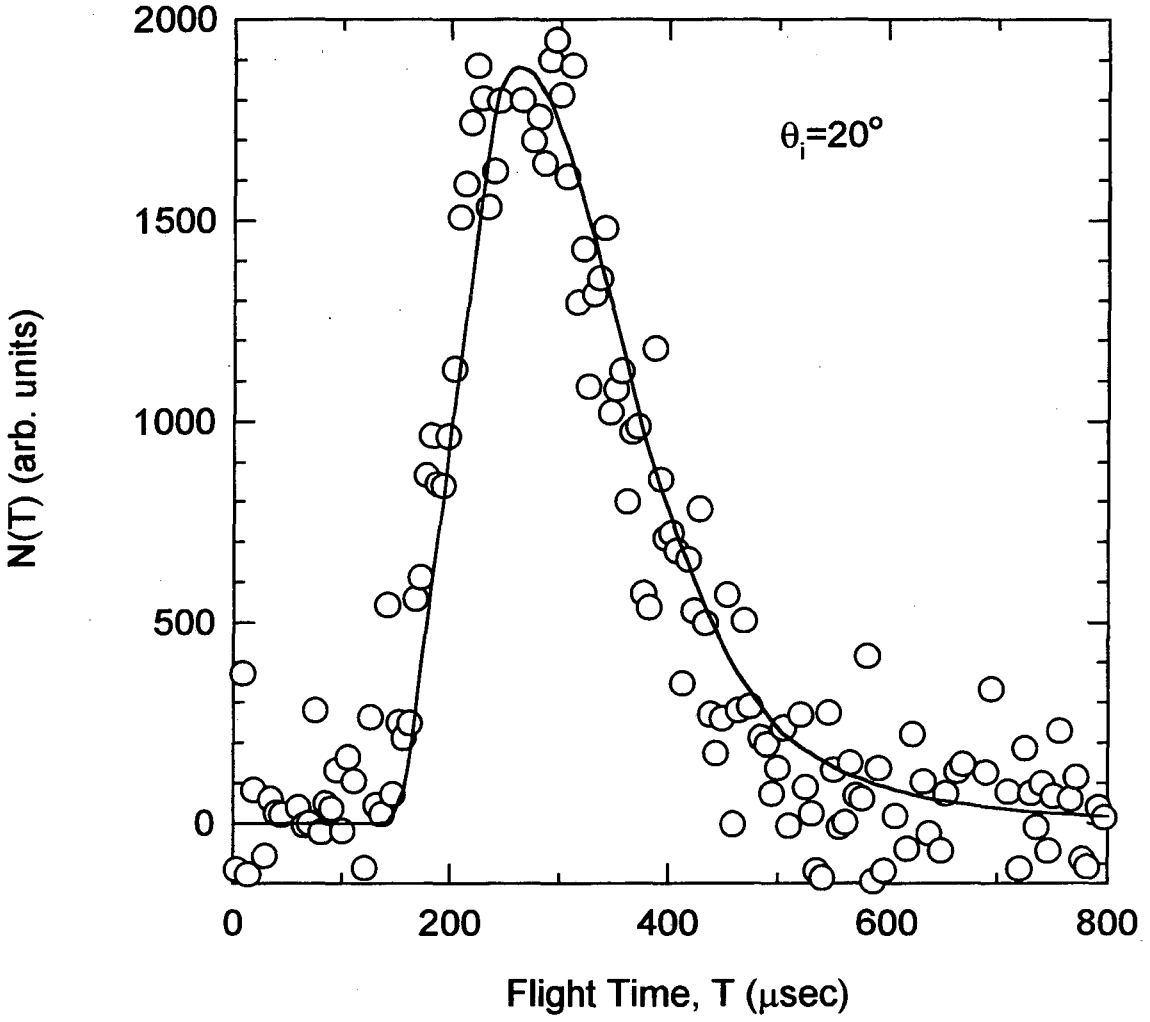

Fig. 10, L. A. Smoliar, J. Chem. Phys.

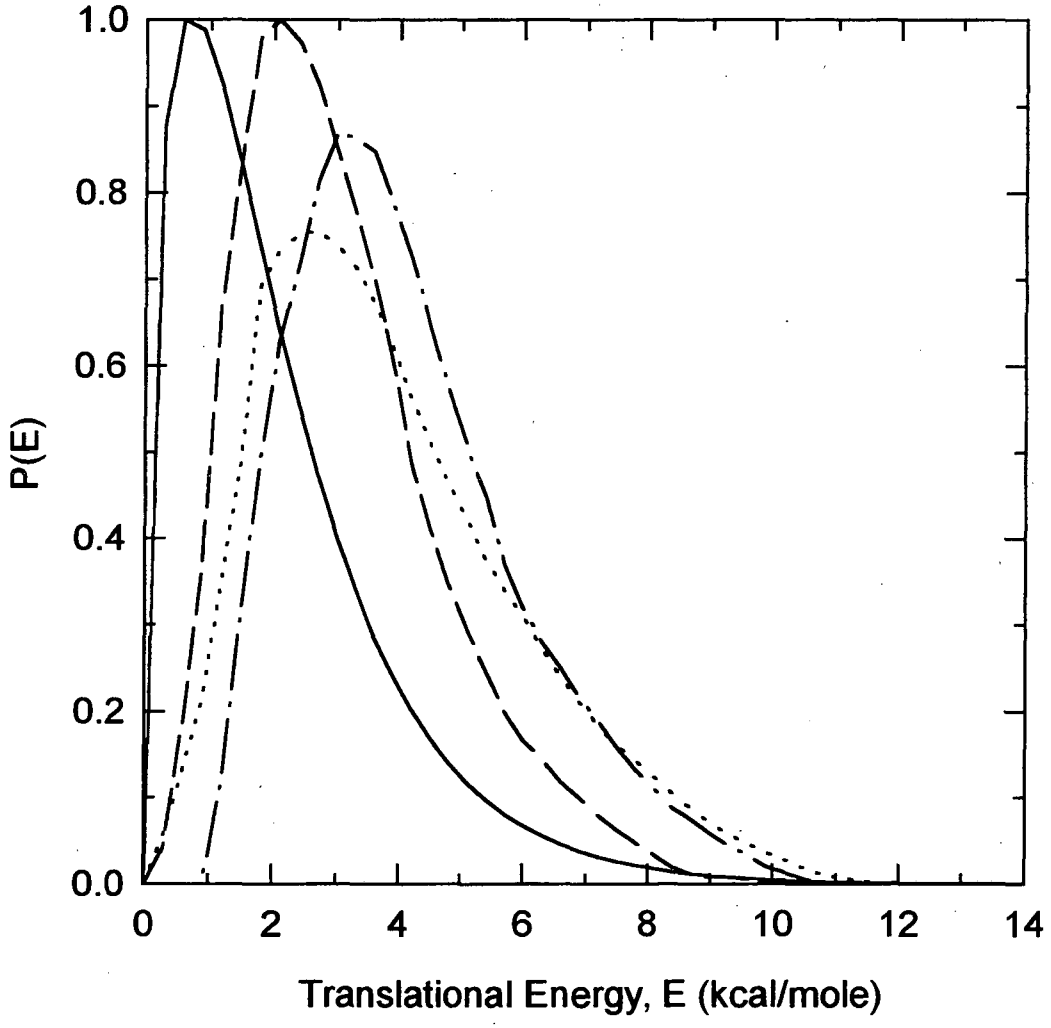

Fig. 11, L. A. Smoliar, J. Chem. Phys.

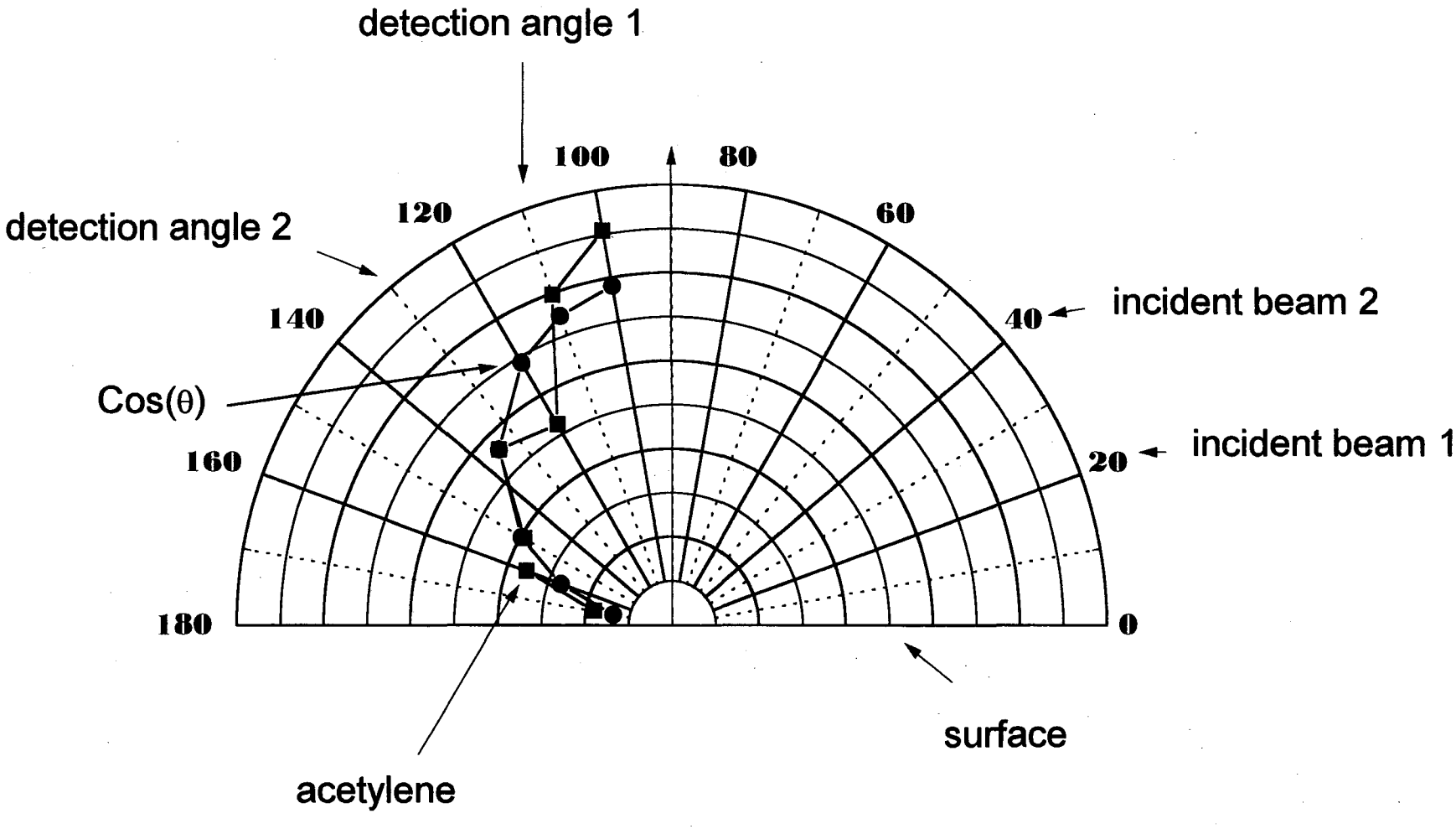

Fig. 12, L. A. Smoliar, J. Chem. Phys.

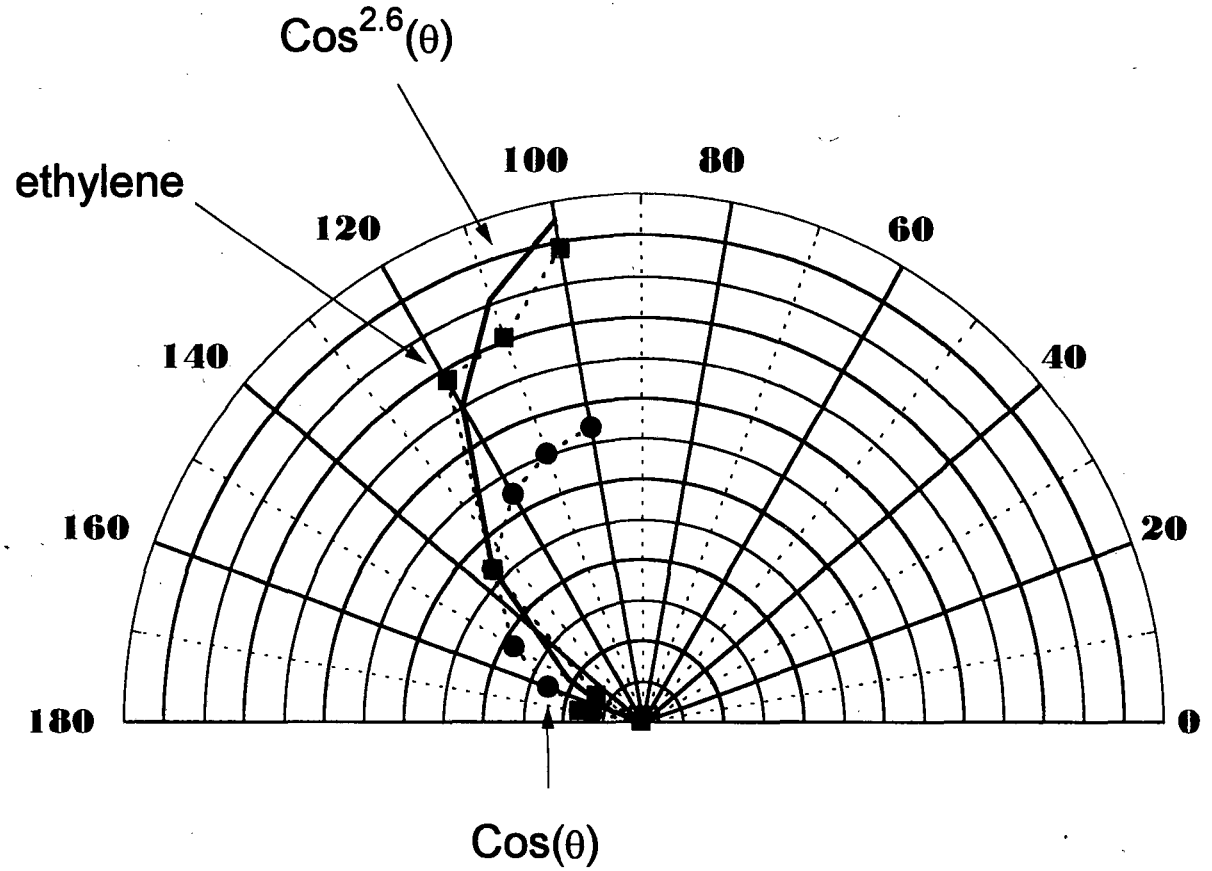

Fig. 13, L. A. Smoliar, J. Chem. Phys.

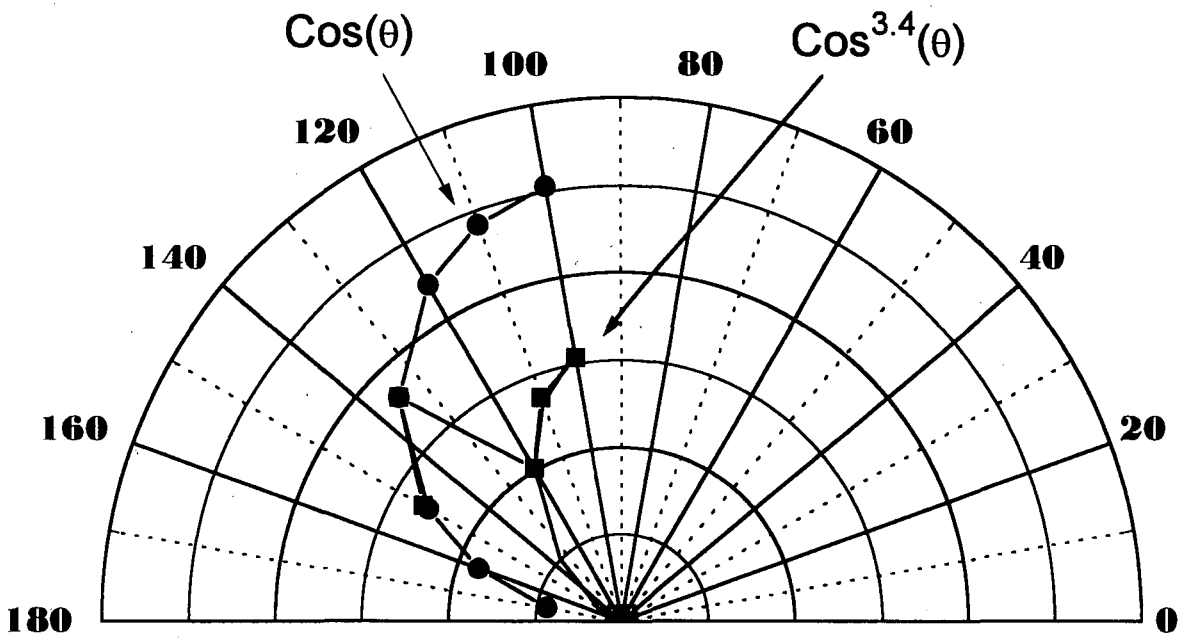

Fig. 14, L. A. Smoliar, J. Chem. Phys.

LAWRENCE BERKELEY LABORATORY
UNIVERSITY OF CALIFORNIA
TECHNICAL INFORMATION DEPARTMENT
BERKELEY, CALIFORNIA 94720